# Static and cyclic indentation of a NiTi shape memory alloy

C. Maletta, F. Furgiuele, E. Sgambitterra
*Dept. of Mechanical Engineering, University of Calabria, 87036 Rende (CS), Italy.*
*carmine.maletta@unical.it*

M. Callisti , B. G. Mellor, R.J.K. Wood
*School of Engineering Sciences, University of Southampton, UK.*
*mc3a09@soton.ac.uk*

**ABSTRACT.** The indentation response of a pseudoelastic nickel-titanium based shape memory alloy (SMA) has been analyzed in this study. In particular, both single quasi static and cyclic indentation tests have been carried out, by using a spherical tip and with indentation loads in the range 50 mN-500 mN, in order to promote large stress-induced transformation zone in the indentation region and, consequently, to avoid local effects due to microstructural variations. The load-displacement data have been analyzed to obtain useful information about the pseudoelastic response of the alloy. To this aim, numerical simulations were developed, by using a commercial finite element (FE) software code, to better understand the microstructural evolution, occurring during indentation process. The results revealed an unusual indentation response of the SMAs, with respect to common metals, and load-displacement data can be advantageously used to analyze their mechanical response.

**SOMMARIO.** Nel presente lavoro è stata analizzata la risposta all'indentazione di una lega a memoria di forma (SMA – Shape Memory Alloy) a base di nickel e titanio. In particolare, sono state eseguite prove di indentazione quasi statiche e cicliche mediante l'utilizzo di un indentatore sferico e per livelli di carico compresi tra 50 mN-500 mN, al fine di favorire la formazione di zone di trasformazione ampie e, pertanto, evitare effetti locali dovuti a variazioni microstrutturali. Le curve carico-spostamento sono state analizzate al fine di ottenere informazioni utili per la comprensione del comportamento pseudoelastico della lega. A tale scopo, sono state condotte analisi numeriche, utilizzando un software commerciale agli elementi finiti, per meglio comprendere i cambiamenti microstrutturali, che avvengono durante il processo di indentazione. I risultati hanno mostrato una risposta inusuale delle SMA, rispetto alle comuni leghe ingegneristiche e, inoltre, le curve forza-spostamento possono essere vantaggiosamente utilizzate per l'analisi della loro risposta meccanica.

**KEYWORDS.** Shape Memory alloys; Indentation tests; Finite element simulations.

## INTRODUCTION

Nickel-Titanium (NiTi) based shape memory alloys (SMAs) have attracted the interest of scientific and engineering community in the last two decades, owing to their unique functional properties, namely pseudoelastic effect (PE) and shape memory effect (SME) [1], coupled with good mechanical performances and biocompatibility. The unique functional responses of NiTi alloys are due to a reversible solid state phase transformation between a parent phase (austenite) and a product phase (martensite), the so called thermoelastic martensitic transformation (TMT). However, despite the increasing interest and the efforts of many researchers to better understand

these unusual mechanisms, the use of NiTi alloys is currently limited to high-value applications (*i.e.* medical devices, MEMS, etc.), due to the high cost of the raw material as well as to the complex component manufacturing; in fact, an accurate control of the processing parameters must be carried out as the functional and mechanical properties of NiTi alloys are significantly affected by the thermo-mechanical loading history experienced during manufacturing. On the other hand, the design of NiTi-based components needs an accurate knowledge of the mechanical and functional response of the material, as well as how this evolves during subsequent thermo-mechanical processes. In addition, most of the NiTi components are characterized by complex shape and small size scale (*e.g.* endovascular stents, micro surgery devices, MEMS, etc.) and their properties cannot be directly obtained from the raw material. Within this context the use of non-destructive techniques to analyze the mechanical and functional properties of small components is essential. Among these techniques nanoindentation is widely used to measure mechanical properties of small volumes of materials with negligible surface damage. However, despite the aforementioned advantages, several difficulties arise in analyzing the mechanical properties of SMAs from the indentation response, due to several micro-structural changes, such as phase transition and grain re-orientation mechanisms. In fact, these latter phenomena are expected to play a significant role in the indentation response of SMAs, as they take place in the indentation region due to the highly localized stresses. As a consequence, several research activities have been carried out to better understand the role of these microstructural changes in the material response, and in most of them the indentation response of NiTi-based films [3-8] and bulk alloys [9-15] has been analyzed. However, notwithstanding the encouraging results obtained in the last years, considerable research needs to be developed for a deeper understanding of the relation between indentation response of SMAs and their mechanical and functional properties.

In this study a commercial pseudoelastic NiTi alloy was analyzed through indentation tests and finite element analysis. In particular, indentations were performed at room temperature by using a diamond tip spherical indenter and loads in the range 50 mN-500 mN, in order to promote large stress-induced transformation zone in the indentation region and, consequently, to avoid local effects due to microstructural variations. Both single quasi static and cyclic indentation tests have been carried out and load-displacement data have been analyzed to obtain useful information about the pseudoelastic response of the alloy. Furthermore, Finite Element (FE) simulations were carried out to the aim of analyzing the stress-induced microstructural mechanisms, occurring in the indentation region, as well as their effects on the indentation response of the SMAs.

## MATERIAL AND METHODS

A Commercial pseudoelastic NiTi sheet (Type S, Memory metalle, Germany), with nominal chemical composition of 50.8 at.% Ni-49.2 at.% Ti and a thickness of 1.5 mm, has been used in this investigation. Fig. 1.a illustrates the DSC thermogram of the raw material together with all transformation temperatures ($M_s$, $M_f$, $A_s$, $A_f$, $R_s$ and $R_f$). The analysis has revealed the presence of a two-stage phase transformation (B2→R→B19') during cooling, with the presence of R-phase (Rhombohedral phase), while a single-stage phase transformation (B2→B19') has been observed during heating. Furthermore, the alloy shows an austenite finish temperature $A_f$=13.7 °C, which indicates a fully austenitic structure at the room temperature. Fig. 1.b illustrates a stress-strain curve of the material, obtained from an isothermal ($T$ = 25 °C) displacement controlled loading-unloading cycle up to a maximum deformation of 6.2%, corresponding to the maximum deformation of the stress-strain transformation plateau. Furthermore, the figure provides the main mechanical parameters of the alloy, in terms of Young's moduli ($E_A$, $E_M$), transformation stresses ($\sigma_{AM}^{s}$, $\sigma_{AM}^{f}$, $\sigma_{MA}^{s}$, $\sigma_{MA}^{f}$) and transformation strain ($\varepsilon_L$), together with the Clausius-Clapeyron constants ($C_A = d\sigma_{MA}/dT$, $C_M = d\sigma_{AM}/dT$).

The indentation response was analyzed by using a nanoindenter NanoTest 600 (Micro Materials Ltd, United Kingdom). Rectangular samples (20mm x 10mm) were cut from the as-received sheet and subsequently polished by using progressively finer grit sandpapers (#800-#4000), and with a diamond compound (5 μm). Both single quasi-static and cyclic indentation tests have been carried out at room temperature, by using a spherical indenter with a tip radius of 25 μm. Indeed, sharp indenters (such as Berkovich, Vickers, atc.), cause high strain gradients, which promotes plastic deformations, increase in dislocation density and, consequently, inhibit the reverse transformation from martensite to the parent phase, as demonstrated previously [11]. Quasi-static tests were executed for increasing values of the maximum load (50, 150, 300 and 450 mN), with a loading/unloading rate of 2.5 $mNs^{-1}$ and for a holding time of 60 seconds at the maximum load. In addition, 20 indentations were carried out for each value of the maximum load, with the aim of capturing an average response of the material. Cyclic tests were executed starting from a maximum load of 50 mN, at the first cycle, up to 500 mN, with an increase of 50 mN per cycle. Furthermore, 10 cyclic indentations were made at the same

loading/unloading rate and holding time of the single tests. Finally, based on the experimental data obtained from cyclic indentation, a representative stress-strain curve was calculated by using the Oliver-Pharr method [2] and the elastic-plastic contact theory, between a sphere and a semi-infinite plane [16-17].

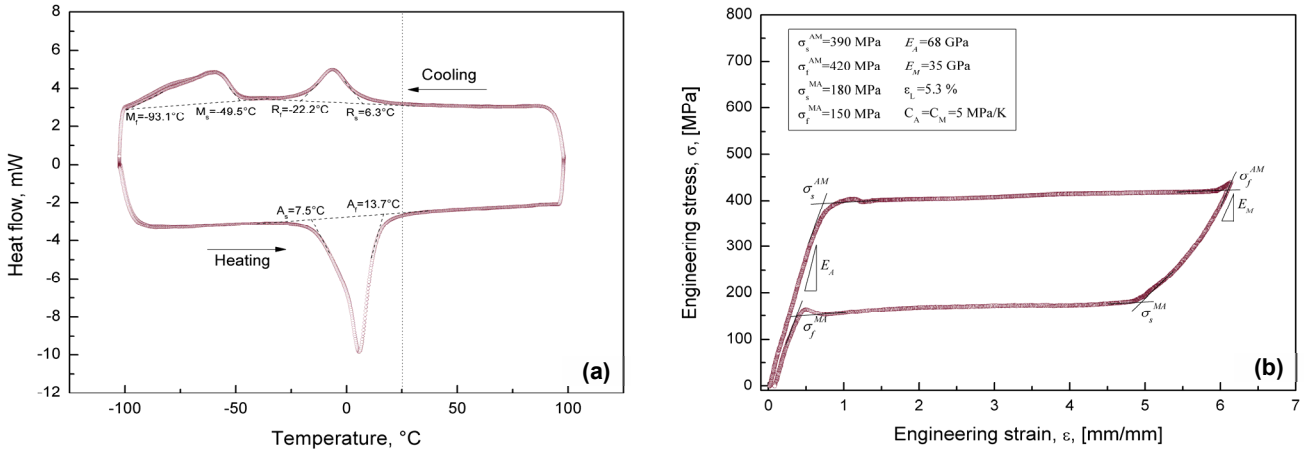


Figure 1: Thermo-mechanical properties of the investigated material: a) DSC thermograph with transformation temperatures and b) Loading-unloading isothermal stress-strain cycle (25 °C).

## NUMERICAL MODELING

Finite Element Analyses (FEA) were carried out, by using a FE commercial software code and a special constitutive model for SMAs [18, 19], in order to study the microstructural evolution during indentation tests. In particular, two-dimensional axisymmetric FE analyses were carried out by modeling a cross-section of the diamond indenter (radius $r$=25 μm, Young's modulus $E$=1141 GPa and Poisson's ratio ν=0.07) and of the sample; this latter was assumed as a cylinder with radius equal to 10 times the diameter of the indenter, in order to avoid boundary effects [17]. The model, illustrated in Fig. 2, consists of about 50400 2D four-node quadrilateral elements. This model results from a preliminary convergence study, while the constitutive model for SMAs, directly implemented in the numerical code, has been calibrated based on the thermo-mechanical parameters illustrated in the previous section.

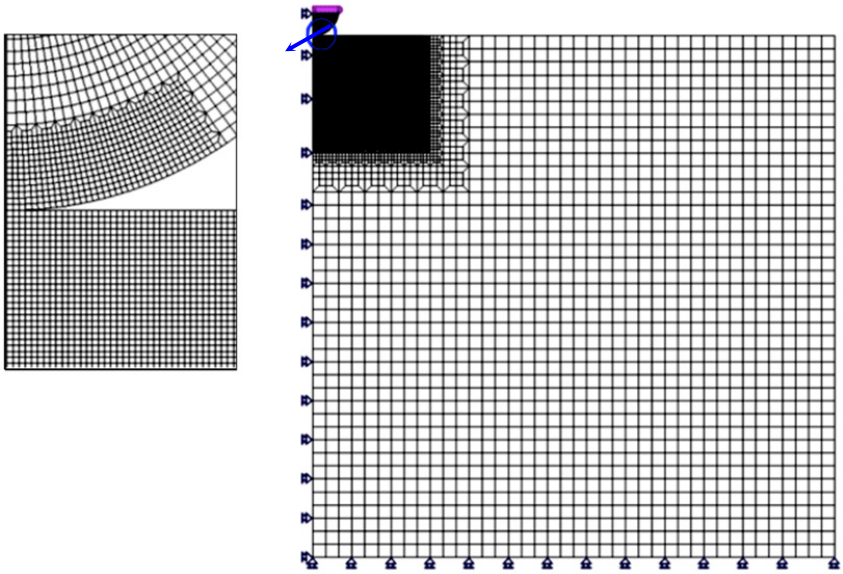

Figure 2: Axisymmetric FE model used to analyze the indentation process.

## RESULTS AND DISCUSSIONS

Preliminary FE studies were carried out to investigate the phase transition mechanisms in the indentation region as well as to better understand the main differences with respect to common elastic-plastic metals. Fig. 3.a illustrates the transformation boundaries in the contact region, obtained from the FE simulation, for a maximum load of 300 mN. In particular, starting from the outer region, a fully untransformed austenitic zone is observed (A), *i.e.* where von Mises stress is below the start transformation stress $\sigma < \sigma_{AM}^{S}$. The area B represents the transformation zone, *i.e.* von Mises stress is in the range between $\sigma_{AM}^{S}$ and $\sigma_{AM}^{f}$ and, consequently, the volume fraction of martensite is between 0 and 1. Finally, C and D are fully transformed martensitic regions, *i.e.* von Mises stress is higher than the transformation stress $\sigma_{AM}^{f}$; however, in C only elastic deformations of the martensitic structure are observed while in D the local stress exceeds yield stress of martensite and permanent deformations are observed. Fig. 3.b illustrates a comparison of the indentation profile between a SMA and an equivalent elastic-plastic material having the same young modulus of the austenitic structure of the SMA and a yield stress equal to the start transformation stress ($\sigma_Y = \sigma_{AM}^{S}$). In particular, the profiles at the maximum load of 300 mN and after unloading, normalized with respect to the maximum depth, are compared. The figure clearly illustrates a smaller residual depth in SMA after unloading, *i.e.* it exhibits higher recovery deformation as a consequence of the reversible stress-induced martensitic transformation in the indentation region.

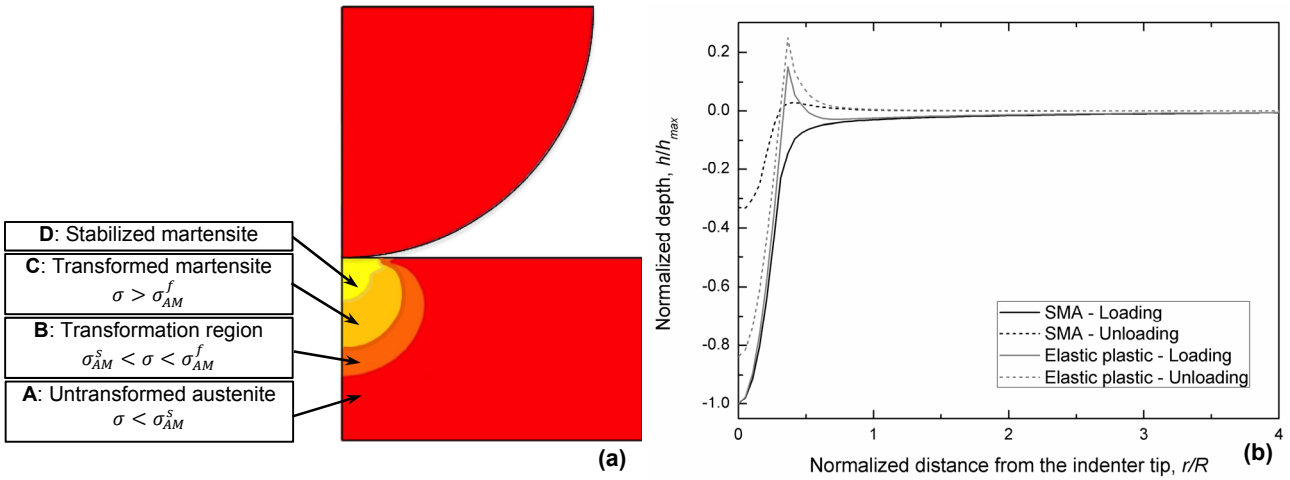


Figure 3: Preliminary FE results: a) stress-induced transformation boundaries near the contact region; b) comparison of the indentation profile between a SMA and an elastic-plastic material.

Fig. 4 shows the load-displacement (P-δ) curves obtained from single quasi-static tests carried out at increasing values of the maximum load: 50 mN (a), 150 mN (b) and 300 mN (c). A good repeatability has been observed in terms of P-δ curves, especially for the higher values of the indentation load, due to a reduction of the experimental errors as well as to a greater amount of material which undergoes phase transformation.

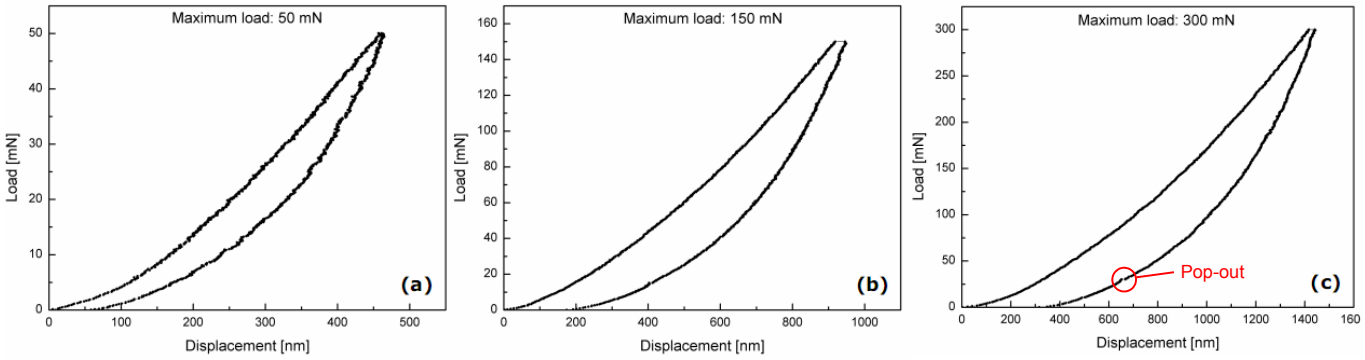


Figure 4: Single quasi-static indentation tests for different values of the maximum load: (a) 50 mN, (b) 150 mN and (c) 300 mN.

The reversible stress-induced phase transition mechanisms are also demonstrated by pop-out events occurring in the unloading stage, which are attributed to the inverse phase transformation from product to parent phase (B19' →B2). In addition, as observed from the preliminary FE simulations, residual depth upon unloading can be analyzed to study the functional behavior of the SMA, in terms of pseudoelastic recovery capability. Fig. 5.a shows the values of the maximum depth ($h_{max}$), residual depth ($h_r$) and residual depth ratio ($h_r/h_{max}$) as a function of the indentation load; the figure illustrates that both residual depth and residual depth ratio increase with increasing indentation load, which indicates an overall reduction of the pseudoelastic response of the SMA, due to the increased fraction of dislocations and stabilized martensite (region D in Fig. 3.a). Similar considerations can be made from an energetic point of view, as illustrated in Fig. 5.b. In particular, this figure illustrates the recovered energy ($E_e$), *i.e.* the energy associated with the unloading path, the dissipated energy ($E_d$), *i.e.* the area between loading and unloading curve, the total energy ($E_t = E_e + E_d$), the recovery energy ratio ($E_e/E_t$) and the dissipated energy ratio ($E_d/E_t$). The figure clearly shows an increase of both dissipated and recovered energy with increasing the indentation load, which indicates an overall increase of both permanent and recovery deformation, as also illustrated in Fig. 5.a; however, the dissipated energy increases more rapidly than the recovery energy which results in an increase of the dissipated energy ratio and an associated decrease of the recovery energy ratio; this result indicates an overall reduction of the pseudoelastic recovery of the SMA when increasing the indentation load.

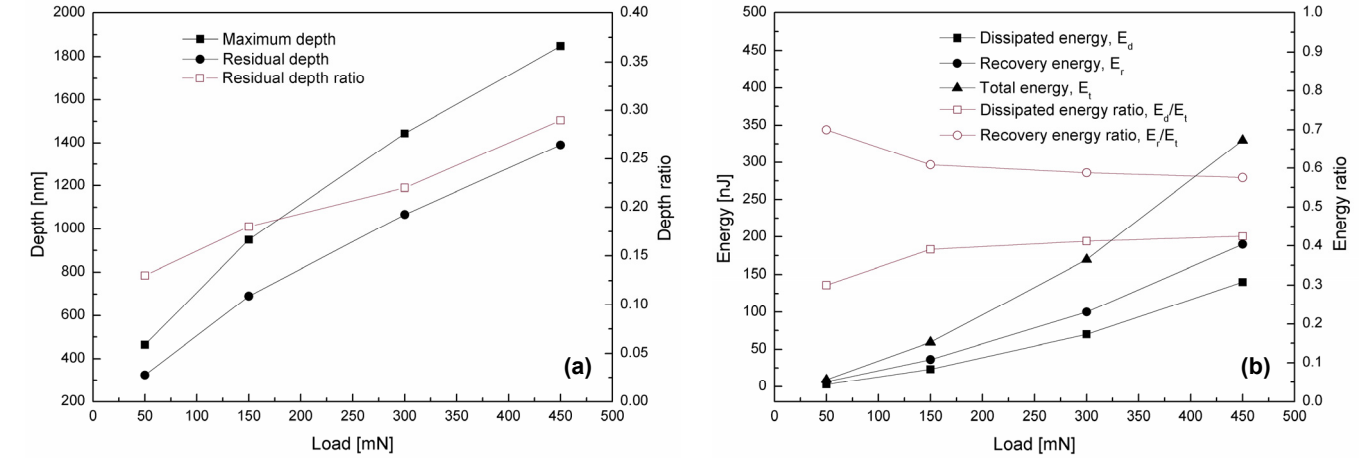


Figure 5. Recovery and residual capability of the SMA after unloading: a) depth recovery and b) recovered energy.

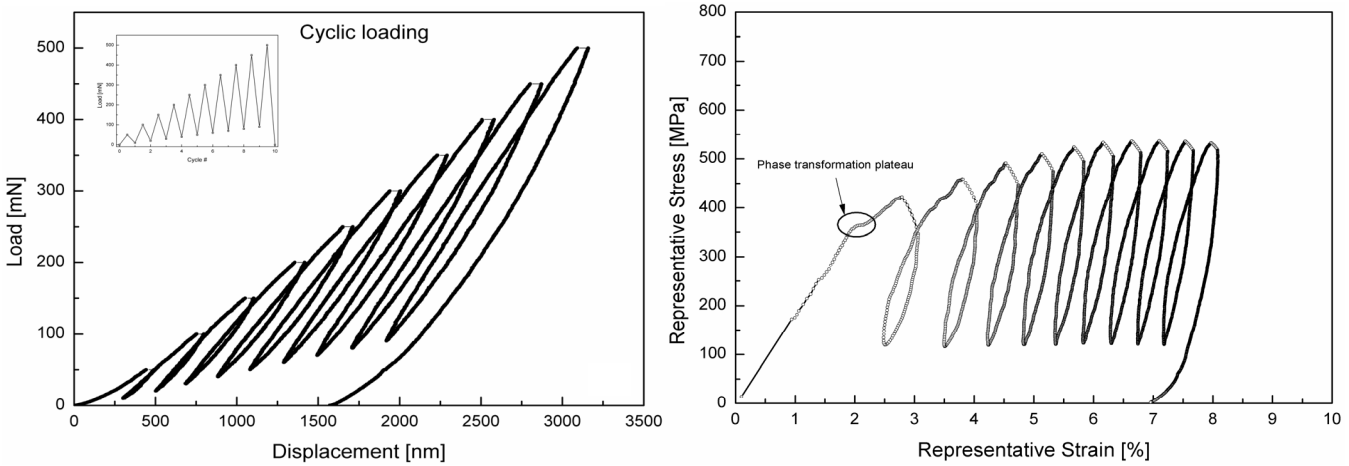


Figure 6: a) Cyclic indentation curves of the SMA for maximum load between 50 mN and 500 mN; b) representative stress-strain curve obtained from cyclic tests by using elastic-plastic contact theory.

Fig. 6.a shows the load-displacement curves obtained from a complete cyclic indentation test for maximum load between 50 mN and 500 mN. The figure clearly shows different paths between the unloading stage of each cycle and the loading stage of the subsequent one and this effect becomes more evident when increasing the maximum load. This phenomenon can be attributed to the stress induced martensitic transformation occurring in the loading path and its reversion during unloading, and can be directly associated with the hysteretic response of the SMA in the stress-strain curve. Fig. 6.b

illustrates a representative stress-strain curve, which was obtained from the cyclic indentation data, by using elastic-plastic contact theory [16, 17]. It is worth noting that this method is based several simplifying assumptions as it does not take into account the phase transition mechanisms in SMAs; however, the obtained curve shows some interesting features which can be advantageously used to analyze the mechanical response of the alloy.
In particular, a stress-induced phase transformation plateau is clearly visible, with a stress value of about 370 MPa at the first indentation cycle, which is close to the direct transformation stress of the alloy (see Fig. 1.b). In addition, an increase of this parameter is observed in the subsequent indentation cycles, which can be attributed to the accumulation of stabilized martensite in the indentation region and, consequently, to an increase of the stress-induced transformation plateau of the alloy. Similar results have been obtained in a previous research [14], and they are of major concern as they provide interesting information about the evolution of transformation stress under repeated mechanical cycles.

## CONCLUSIONS

The indentation response of a pseudoelastic NiTi shape memory alloy were analyzed in this study, by experimental measurements and numerical simulations. Both single quasi static and cyclic indentation tests were carried out and load-displacement curves were analyzed to study the pseudoelastic response of the alloy. In addition, numerical simulations were developed to better understand the microstructural evolution occurring during indentation process. The main results of this study can be summarized as follows:

- Stress induced transformation mechanisms occur in the indentation region, as demonstrated by preliminary FE simulations, which significantly affect the indentation response of SMAs with respect to common metals;
- Spherical indenter should be used, in order to promote large stress-induced transformation zone in the indentation region and, consequently, to avoid local effects due to microstructural variations;
- The fraction of dislocations and stabilized martensite beneath the indenter increases with increasing the indentation load in single quasi-static tests, which results in an overall reduction of the recovery capability after unloading;
- Cyclic indentation tests, carried out at increasing values of the indentation loads, should be used to identify the characteristic transformation stress of the alloy.

## REFERENCES

[1] K. Otsuka, X. Ren, Progr. Mater. Sci. 50 (2005) 511.
[2] W.C. Oliver, G.M. Pharr, J. Material Res. 7 (1992) 1564.
[3] G. Satoh, A. Birnbaum, Y.L. Yao, In: Proc. Of Int. Congress on Applications of Lasers and Electro-Optics, Temecula CA (2008).
[4] P.D. Tall, S. Ndiaye, A.C. Beye, Z. Zong, W.O. Soboyejo, H.J. Lee, A.G. Ramirez, K. Rajan, Mater. Manuf. Processes, 22 (2007) 175.
[5] A.K. Nanda Kumar, C.K. Sasidharan Nair, M.D. Kannan, S. Jayakumar, Mater. Chem. Phys. 97 (2006) 308.
[6] G.A. Shaw, W. C. Crone, Mater Res Soc Symp Proc., 791 (2003) 215.
[7] W.C. Crone, G.A. Shaw, D.S. Stone, A.D. Johnson, A.B. Ellis, In: Society for Experimental Mechanics, SEM Annual Conference Proceedings, Carlotte, NC (2003).
[8] G.A. Shaw, D.S. Stone, A.D. Johnson, A.B. Ellies, W.C. Crone, Appl. Phys. Lett., 83 (2003) 257.
[9] C. Liu, Y.P. Zhao, T. YU, Mater. Design, 26 (2005) 465.
[10] C. Liu, Y. Zhao, Q. Sun, T. YU, Z. Cao, J. mater. Sci. 40 (2005) 1501.
[11] A.J. Muir Wood, T.W. Clyne, Acta Materialia 54 (2006) 4607.
[12] A.J. Miur Wood, J.H You, T.W. Clyne, Proc. SPIE 5648, art. no. 39 (2205) 216.
[13] W. Yan, Q. Sun, X.Q. Feng, L. Qina, Int. J. Solids Struct. 44 (2007) 1.
[14] M. Arciniegas, Y. Gaillard, J. Pena, J.M. Manero, F.J. Gil, Intermetallics 17 (2009) 784.
[15] R. Liu, D.Y. Li, Scripta Materialia, 41(7) (1999), 691.
[16] K.L. Johnson, Contact Mechanics, Cambridge University Press (1985).
[17] A.C. Fisher-Cripps, Nanoindentation, Second Edition, Springer (2002).
[18] M. Saeedvafa, "A Constitutive Model for Shape Memory Alloys", Internal MSC Report (2002).
[19] M. Saeedvafa, R.J Asaro, LA-UR-95-482, Los Alamos Report, (1995).